Preliminary Results from Engineering Seismological Studies of the Central Weather Bureau's Free-Field Ground Motion Recordings in Taiwan

Yi-Ben Tsai[1], Yih-Min Wu[1,2], Kun-Sung Liu[1,2], and Tzay-Chyn Shin[2]

1. Institute of Geophysics, National Central university, Chungli, Taiwan, ROC
2. Central Weather Bureau, Taipei, Taiwan, ROC

ABSTRACT

Several hundreds of high-resolution wide-dynamic-range digital horizontal-component accelerograms obtained by the Taiwan Strong Motion Instrumentation Program from three moderate, shallow earthquakes in northeastern and southwestern Taiwan are analyzed. The analyses are focused on three engineering seismological topics on local magnitude, M_L, determination, attenuation of peak ground acceleration, and regional variations of response spectral shapes. Preliminary results can be summarized as follows:

1. The M_L magnitude is determined to be 5.89 for the 12/15/93 earthquake, 6.41 for the 6/5/94 earthquake, and 6.39 for the 6/25/95 earthquake, respectively.
2. Synthetic Wood-Anderson seismograms indicate that the existing distance correction function for M_L determination for Taiwan earthquakes may result in overestimates of M_L for distances greater than 100 km and underestimates for small distances.
3. Observed horizontal peak ground accelerations (PGA) indicate that the existing attenuation relation may result in underestimates of PGA, especially at small distances.
4. There are significant regional variations in the normalized response spectral shape. Sites in northern Taiwan on average have larger response for frequencies below 4 to 5 Hz than sites in southwestern Taiwan. Moreover, Taipei Basin possessed prominent spectral peaks centered at frequencies from 1 to 1.2 Hz, and from 0.4 to 0.5 Hz, respectively.

Introduction

Since 1993 the Seismological Center of the Central Weather Bureau has undertaken a major strong motion instrumentation program in Taiwan (Liu et al., 1994). Thus far, a total of 624 high-resolution wide-dynamic-range digital accelerographs have be installed at free-field sites throughout the densely populated areas of Taiwan. Thousands of high-quality digital accelerograms were collected from numerous earthquakes occurred in the last few years. These new recordings provide an excellent database for making various engineering seismological studies. In this paper we present preliminary results from analyzing recordings from three moderate, shallow earthquakes to study some aspects related to local magnitude determination, peak ground acceleration attenuation, and response spectral shapes.

The three earthquakes were the December 15, 1993 earthquake in southwestern Taiwan, the June 5, 1994 and June 25, 1995 earthquakes in northeasten Taiwan. Relevant hypocentral information about these earthquakes is given in Table 1. At the time of 12/15/93 M_L 5.89 earthquake, recordings were obtained from 160 of the 393 operational accelerograph sites. The locations of these recording and operational sites are shown in solid and open circles, respectively, in the left part of Figure 1. The epicenter was at southwestern Taiwan, as shown in the figure by an open star. The focal depth of this earthquake was 12.5 km. Most of the recording sites for this earthquake were located in southwestern Taiwan south of 24.5°N.

During the 6/5/94 M_L 6.41 earthquake, recordings were obtained at 249 of the 394 operational accelerograph sites. As shown in the middle part of Figure 1, all recording sites for this earthquake were located north of 23°N. Its epicenter was located on the northeastern coast of Taiwan. The focal depth was 5.3 km. Lastly, recordings were obtained at 337 of the 609 operational accelerograph sites from the 6/25/95 M_L 6.39 earthquake. As shown in the left part of Figure 1, most recording sites for this event were located north of 23°N, just like the 6/5/94 earthquake. Its epicenter was located just outside the southern edge of the Lanyang Plain. The focal depth was 39.9 km for this event.

It is remarkable that the recording sites for all three earthquakes were distributed all over the whole distance range from very near the epicenters out to as far as 250 km . Moreover,

among the three events there were numerous overlapping recording sites located in western Taiwan from 23°N to 24.5°N. The combined data set of the three moderate, shallow earthquakes provides a dense coverage of practically all populated areas of Taiwan proper, with an only exception of southernmost part of Taiwan.

These excellent features of site coverages make the recordings particularly suitable for reevaluating several elementary engineering seismological aspects. In order to take advantage of the new opportunity, we first used the recordings of the horizontal components to obtain the synthetic Wood-Anderson seismograms not only to determine the local magnitudes(M_L) of the earthquakes but also to refine the distance correction function, -logAo for M_L calculation. Next, we used the recorded horizontal peak ground acceleraions (PGA), along with the newly improved M_L values to modify the attenuation relations proposed previously for Taiwan area. Finally, we calculated the normalized response spectral shapes to study regional differences in ground motion frequency characteristics. Preliminary results from these studies are presented below.

Local Magnitude Determination

Local magnitude M_L has become widely used by both seismologists and the general public to describe the size of earthquakes since it was initially introduced by Richter (1935). As originally defined, M_L is determined from the amplitude of motion recorded by the standard Wood-Anderson seismograph, which has a natural period of 0.8 sec, a damping constant of 80 percent of critical, and a magnification of 2800. The period and damping of the Wood-Anderson instrument are such as to make it sensitive to ground motion in the period range of greatest engineering interest. As succinctly stated by Jennings and Kanamori (1983), this feature, plus the fact that M_L is determined from ground motions closer to the source than is the case for other magnitudes, means that M_L is of particular interest for most engineering applications.

Unfortunately, Wood-Anderson seismographs are antiquated and are not in widespread use outside of southern California. Even where available, the limited dynamic range of about 50 dB of the W-A seismograph severely limits the magnitude range for which M_L can be estimated. Thus, seismologists often use an alternative technique for estimating M_L when W-A records are not available by transforming the signals recorded on modern seismographs into "synthetic W-A seismograms" and making the measurements and computations prescribed by Richter (1958) (Bakun and Lindh, 1977; Kanamori and Jennings, 1978). Previous experiments have demonstrated directly that accurate synthetic W-A seismograms can indeed be derived from a modern seismograph by comparing with actual W-A seismograms recorded on the same pier (Bakun, Houck, and Lee, 1978).

The synthetic W-A seismogram is the record that would have been written at the site of of a modern seismograph as if a W-A seismograph (with appropriate gain and dynamic range) had been in operation there. The free-field ground acceleration recordings from the high-resolution wide-dynamic-range digital accelerographs in the CWB strong motion network are ideal for deriving synthetic W-A seismograms because they can record on scale even the strongest ground motions, yet at the same time provide enough resolution for weak ground motions from small earthquakes or at large distances. Mathematically, the relation between a synthetic W-A seismogram and a ground acceleration recording can be expressed by

$$\ddot{x}(t) + 2h\omega_0\dot{x}(t) + \omega_o^2 x(t) = -a(t) \quad \text{---- (1)}$$

where h = 0.8 is damping constant, $\omega_0 = 2\pi / 0.8$ is angular frequency, x(t) is the synthetic W-A seismogram at a magnification of unity, and $a(t)$ is the ground acceleration. Equation 1 can be solved for $x(t)$ for a given $a(t)$ in the time domain by numerical integration or in the frequency domain by Fast Fourier Transform (FFT) and inverse FFT. In the present study we opted for the latter approach. Thus, Equation 1 can be transformed into the frequency domain as follows:

$$(i\omega)\cdot(i\omega)\cdot X(\omega) + 2h\omega_0\cdot(i\omega)\cdot X(\omega) + \omega_0^2\cdot X(\omega) = -A(\omega) \quad \text{----(2)}$$

where $X(\omega)$ and $A(\omega)$ are the Fourier transforms of $x(t)$ and $a(t)$, respectively. We have used the relations $\ddot{X}(\omega) = (i\omega)\cdot(i\omega)\cdot X(\omega)$ and $\dot{X}(\omega) = (i\omega)\cdot X(\omega)$. We can obtain $X(\omega)$ from Equation 2,

$$X(\omega) = \frac{A(\omega)}{(\omega^2 - \omega_0^2) - 2h \cdot \omega_0 \cdot (i\omega)} = H(\omega) \cdot A(\omega) \quad \text{----(3)}$$

Where $H(\omega)$ represents the complex response function of a W-A seismograph with respect to an acceleration input. The amplitude and phase response functions of $H(\omega)$ are shown in the upper part of Figure 2. From these plots it is evident that $H(\omega)$ has the properties of a low-pass filter. In other words, the synthetic W-A seismogram is just a low-pass filtered accelerogram with a cut-off frequency of 1.25 Hz. It should be noted that there is an accompanying phase change of π at low frequencies. These features can be seen clearly from an example shown at the lower part of Figure 2. The input accelerogram was one of the recordings from the 6/5/94 earthquake. The resultant synthetic W-A seismogram was obtained by performing IFFT on $X(\omega)$. We find from the figure that the synthetic W-A waveform is basically a low-pass filtered version of the input accelerogram with a reversed polarity.

We have applied the above procedure to all horizontal accelerograms from the three earthquakes to obtain the corresponding synthetic W-A seismograms. The associated W-A amplitudes are then obtained by multiplying the peak values (in mm) from the W-A seismograms with a magnification factor of 2800. The logarithm of W-A amplitudes are plotted in Figure 3 as function of hypocentral distances in the upper left part for the 12/15/93 earthquake, in the lower left part for the 6/5/94 earthquake, and in the upper right part for the 6/25/95 earthquake, respectively. Also shown in these plots are the best-fit curves through the data points. From these plots we find that a linear log A vs log R curve can fit the data points quite well. The corresponding M_L values are 5.89, 6.41 and 6.39 for the 12/15/93, 6/5/94 and 6/25/95 earthquakes, respectively. It is also interesting to note that the log A values in the Taipei Basin area at R between 50 and 75 km for the 6/5/94 and 6/25/95 earthquakes are generally higher than the average. This indicates that there is significant ground motion amplification in the basin.

At the lower right part of Figure 3, we compare the three observed best-fit curves, after anchoring them at the point Δ = 100 km and log Ao = -3, with the corresponding curves proposed for southern California (Hutton and Boore, 1987) and for Taiwan (Shin, 1993). It is seen that the new curves from the three Taiwan earthquakes consistently lie above the previously published curves at hypocentral distances greater than 100 km. At a distance of 250 km, the difference in log Ao could reach 0.4. In other words, the existing log Ao functions will result in too large corrections for distance effect in estimating the M_L. At small hypocentral distances, the newly observed curves are in agreement with the southern California curve, but are below the existing Taiwan curve. In summary, the very excellent new ground motion data can be used to refine the log Ao function for M_L determination in Taiwan.

Attenuation of Horizontal Peak Ground Accelerations

The first step in defining ground motions for seismic design usually is to estimate the horizontal peak ground accelerations (PGA) from given attenuation relations as function of earthquake magnitude and distance. Thus, it is important to review periodically the PGA attenuation relations as new ground motion data become available and to make appropriate revisions. For Taiwan it is good time to do so now becauase of the recent availability of numerous high-quality recordings produced by the CWB strong motion instrumentation program. Here we present preliminary findings from studying the PGA data sets of the three moderate, shallow earthquakes.

Figure 4 shows the observed horizontal PGA values as function of hypocentral distance for the 12/15/93 M_L5.89 earthquake in the upper left part, for the 6/5/94 M_L6.41 earthquake in the lower left part, and for the 6/25/95 M_L6.39 earthquake in the upper right part of the figure, respectively. For each earthquake a best-fit attenuation curve through the data points is also found. From these plots we find that the attenuation relations can be nicely represented by linear log PGA vs log R curves. This implies that log W-A vs log PGA would also follow a linear relation. This is really not surprising in view of the fact that the W-A waveform is a low-pass filtered version of the acceleration waveform. It is interesting again to point out that the PGA values in the Taipei Basin area (at distances between 50 and 75 km) are higher than the average for both the 6/5/94 and 6/25/95 earthquakes. Particularly for the 6/25/95 earthquake, the PGA values in the Lanyang Plain area (at distances 40 to 50 km) are also higher than the average, again indicating basin amplification effects on ground motions.

At the lower right part of Figure 4 we compare the best-fit attenuation curves for the three earthquakes with the attenuation curves for M_L6.0 and M_L6.5 as calculated from the formula previously proposed by Loh (1995). It is found that the existing attenuation curves tend to give lower PGA values than the observed ones, especially at small distances. In other words, we need to refine the existing horizontal PGA attenuation relations in order to represent better the actual data.

Normalized Response Spectral Shapes

In engineering contexts, because of the interest in the motion of buildings and other engineered structures, the main attention is given to the response of a simple damped linear oscillator due to forcing accelerations. For design purposes, it is often sufficient to know only the maximum value of the response of the structure to seismic input. Thus, in terms of the simple oscillator model, Housner (1941) defined the response spectrum as the curve of maximum response of oscillators with different frequencies to the given input ground motion. In order to examine more closely the frequency dependency of the response spectrum, the latter is often normalized by the PGA value of the input ground motion to produce the corresponding response spectral shape. Average response spectral shapes are then obtained from a large suite of ground motion recordings to represent average frequency characteristics of ground motion. Simplified versions of these average spectral shapes are then devised and incorporated in building codes for seismic design purposes, such as the Uniform Building Code (ICBO, 1994).

We have calculated the normalized response spectral shapes at 5% damping from hundreds of horizontal-component accelerograms from the three earthquakes. We further calculated the average spectral shapes of the NS and EW components, separately, for each earthquake. The results are shown in the upper part of Figure 5. From this plot we find first that the average spectral shapes are quite similar between the NS and EW components for all three earthquakes. Second, we find that the average response spectral shapes from the recordings of the 12/15/93 earthquake in southwestern Taiwan differ significantly from those of the 6/5/94 and 6/25/95 earthquakes in northern Taiwan. The latters have larger response at lower frequencies than the former. The cross-over frequencies are between 4 and 5 Hz. Thus, there is clear evidence for significant regional variations in response spectral shape between northern and southwestern Taiwan.

The enhanced response at lower frequencies in northern Taiwan is due largely to the amplification effects of the Taipei Basin and Lanyang Plain, particularly the former. To demonstrate this point we calculated separate average response spectral shapes from recordings in the Taipei Basin and compare them with the overall average response spectral shapes for the 6/5/94 earthquake in the middle part and for the 6/25/95 earthquake in the lower part of Figure 5, respectively. For both earthquakes we find prominent response spectral peaks centered at 1 to 1.2 Hz. In addition, there is a second group of response spectral peaks centered at 0.45 Hz for the 6/5/94 earthquake. These data indicate that buildings of 8 to 10 stories high and of 21 stories high in Taipei Basin will respond more strongly to seismic motions due to the amplification effects of the basin. This effect was incorporated in the revised seismic design spectrum by Tsai et al. (1991) following the November 15, 1986 earthquake near Hualien. In light of the new data and of its importance, a more thorough review of this aspect seems warranted.

References

Bakun, W.H. and Lindh, A.G. (1977). Local magnitudes, seismic moments and coda durations for earthquakes near Oroville, California, Bull. Seism. Soc. Am., v67, 615-629.

Bakun, W.H., Houck, S.T., and Lee, W.H.K. (1978). A direct comparison of "synthetic" and actual Wood-Anderson seismograms, Bull. Seism. Soc. Am., v68, no.4, 1199-1202.

Housner, G.W. (1941). Calculating the response of an oscillator to arbitrary ground motion, Bull. Seism. Soc. Am., v31, no.2, 143-149.

Hutton, L.K. and Boore, D.M. (1987). The ML scale in Southern California, Bull. Seism. Soc. Am., v77, no.6, 2074-2094.

International Conference of Building Officials (1994). Uniform Building Code, International Conference of Building Officials, Whittier, California.

Jennings, P.C. and Kanamori, H. (1983). Effect of distance on local magnitudes found from strong-motion records, Bull. Seism. Soc. Am., v73, no.1, 265-280.

Kanamori, H. and Jennings, P.C. (1978). Determination of local magnitude, ML, from strong-motion accelerograms, Bull. Seism. Soc. Am., v68, no.2, 471-485.

Liu, K.S., Shin, T.C., Lee, W.H.K., and Tsai, Y.B. (1993). Taiwan Strong Motion

Instrumentation Program - The characteristic comparison of free-field accelerographs (in Chinese). Meteorological Journal of the Central Weather Bureau, v.39, no.3, 132-150.

Loh, C.H., J.Y. Hwang and T.C. Shin (1996). Observed variations of earthquake motiom across a basin-Taipei Basin, Submitted for publication on Earthquake Spectra.

Richter, C.F. (1935). An instrumental earthquake magnitude scale, Bull. Seism. Soc. Am., v25, no.1, 1-32.

Richter, C.F. (1958). Elementary Seismology, W.H. Freeman, San Francisco, 768 pp.

Shin, T.C. (1993). The calculation of local magnitude from the simulated Wood-Anderson seismograms of short-period seismograms in the Taiwan area, Terrestrial, Atmospheric, and Oceanic Sciences, v4, no.2, 155-170.

Tsai, I.C., Chiu, C.P., Tsai, K.C., and Hsiang, W.P. (1991). Studies on seismic input provisions for revision of the building code (in Chinese), Chinese Structural Engineer's Association.

Table 1. List of earthquakes studied

No.	Date	Lon.	Lat.	Depth (km)	ML (CWB)	ML (This study)
1	12/15/1993	120.52	23.21	12.5	5.7	5.89
2	06/05/1994	121.84	24.46	5.3	6.2	6.41
3	06/25/1995	121.67	24.61	39.9	6.5	6.39

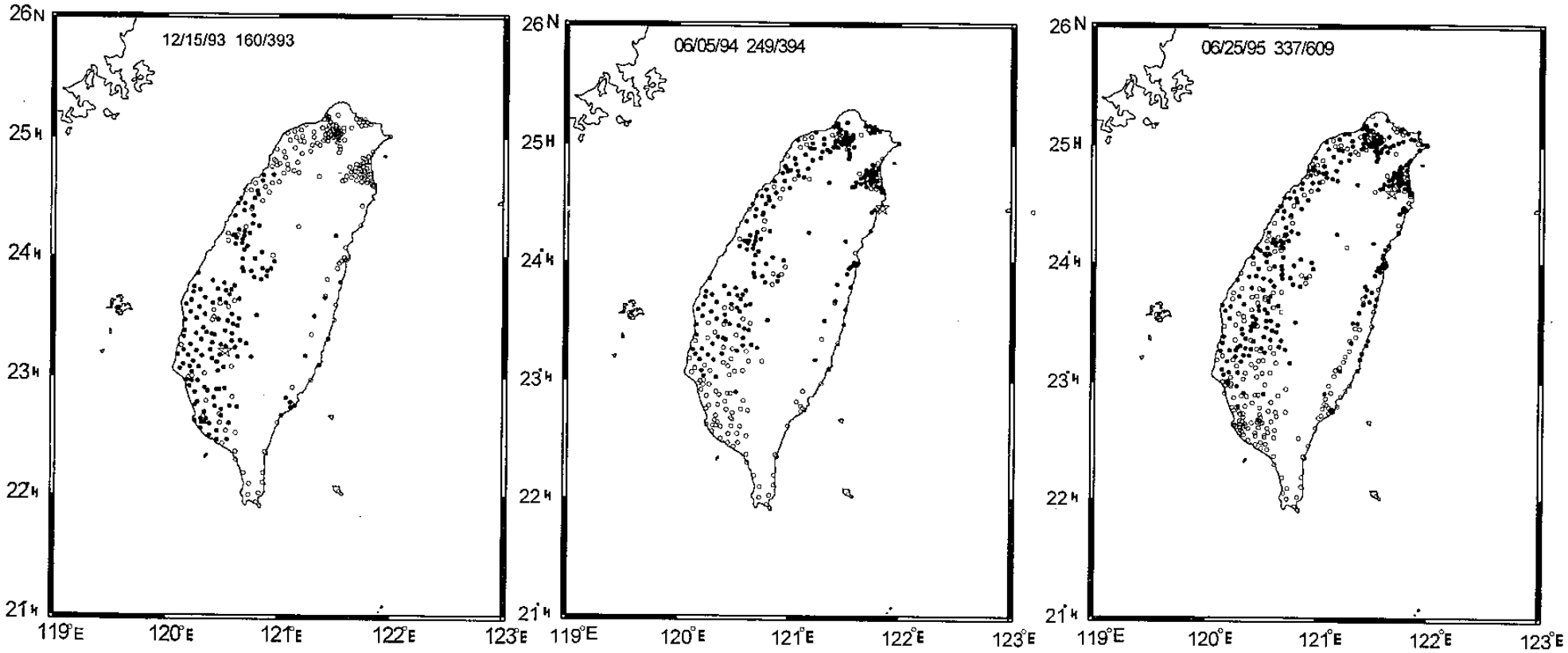

Figure 1. Locations of the epicenter (open star), operational accelerograph site (open circle), and recording accelerograph site (soid circle): From left to right for the 12/15/93 earthquake, the 6/5/94 earthquake, and the 6/25/95 earthquake, respectively.

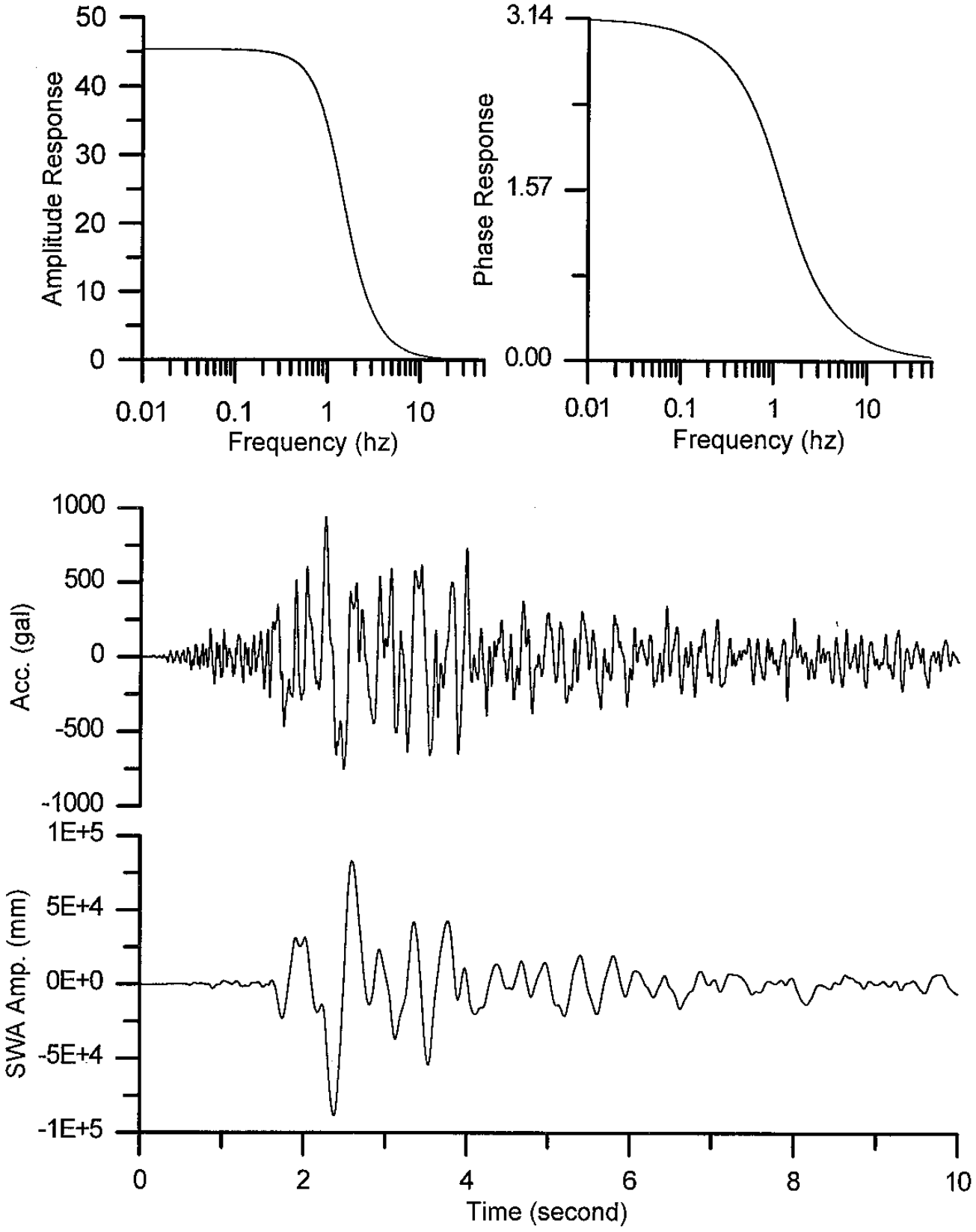

Figure 2. Top: Amplitude and phase response functions of the Wood-Anderson seismograph with respect to a ground acceleration input.
Bottom: Example of a ground acceleration input waveform and the resultant synthetic Wood-Anderson seismogram.

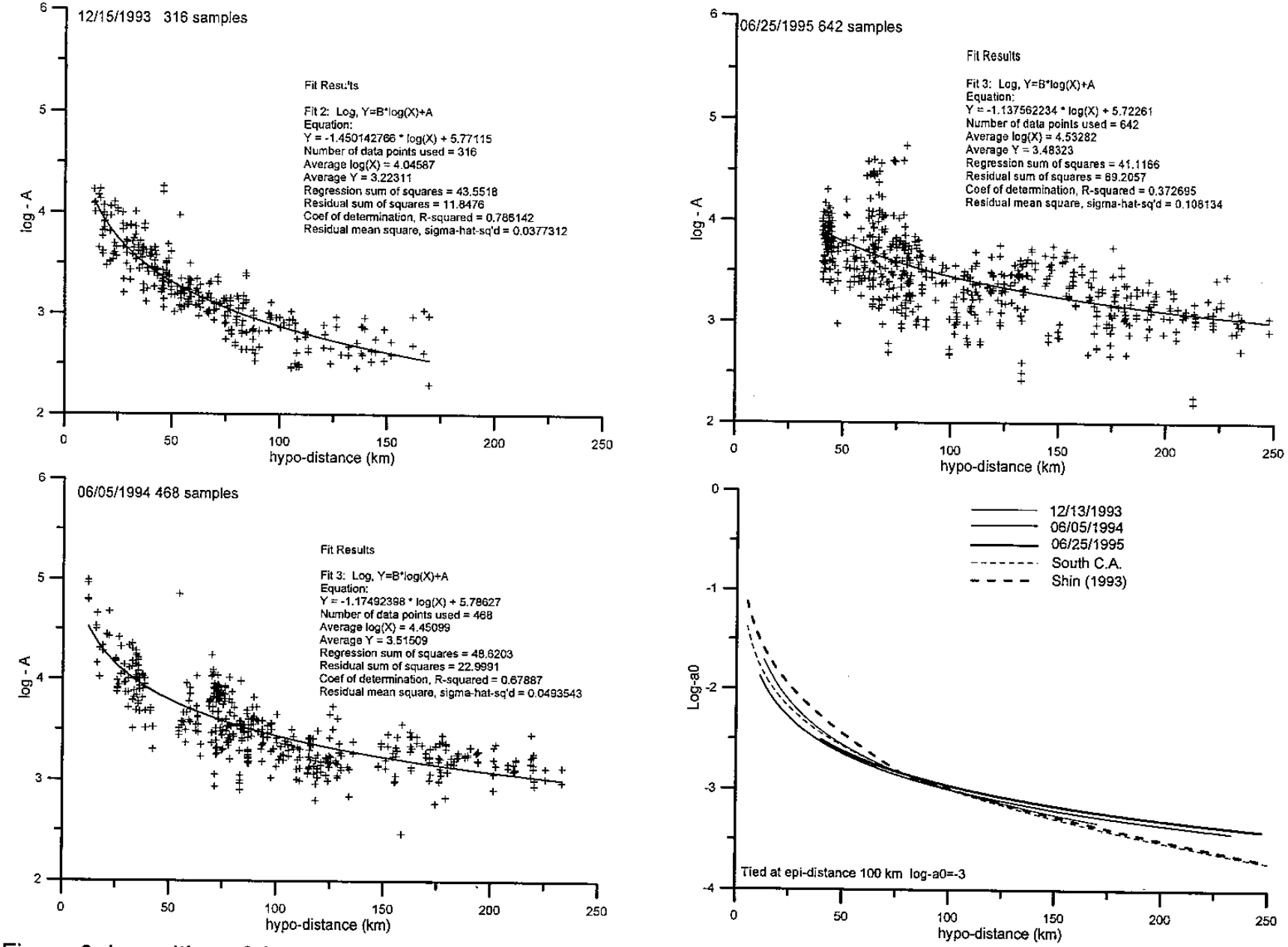

Figure 3. Logarithm of the synthetic Wood-Anderson amplitude as function hypocentral distance: upper left for the 12/15/93 earthquake, lower left for the 6/5/94 earthquake, upper right for the 6/25/95 earthquake, and lower right for the best-fit curves, respectively.

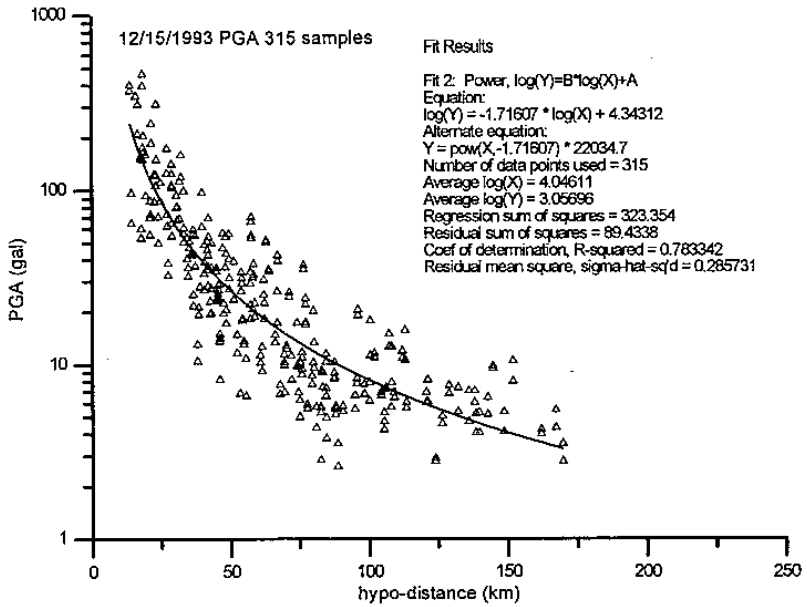

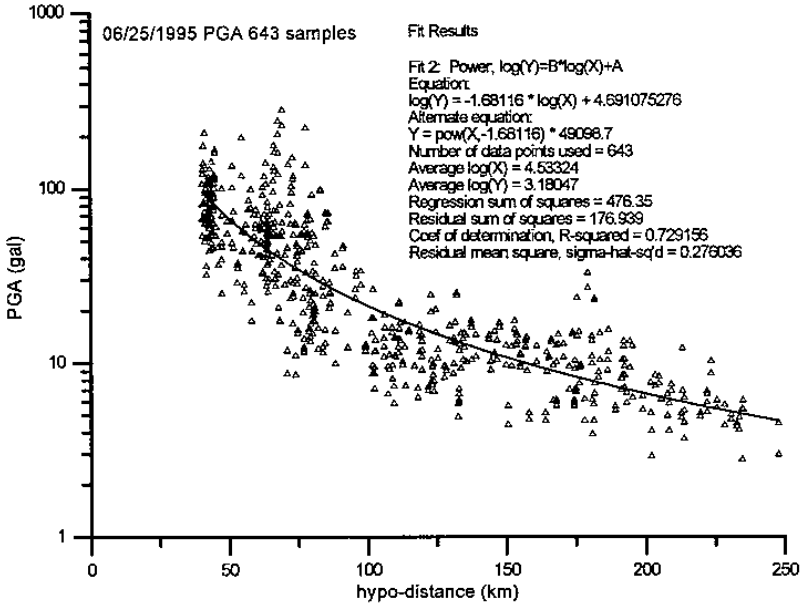

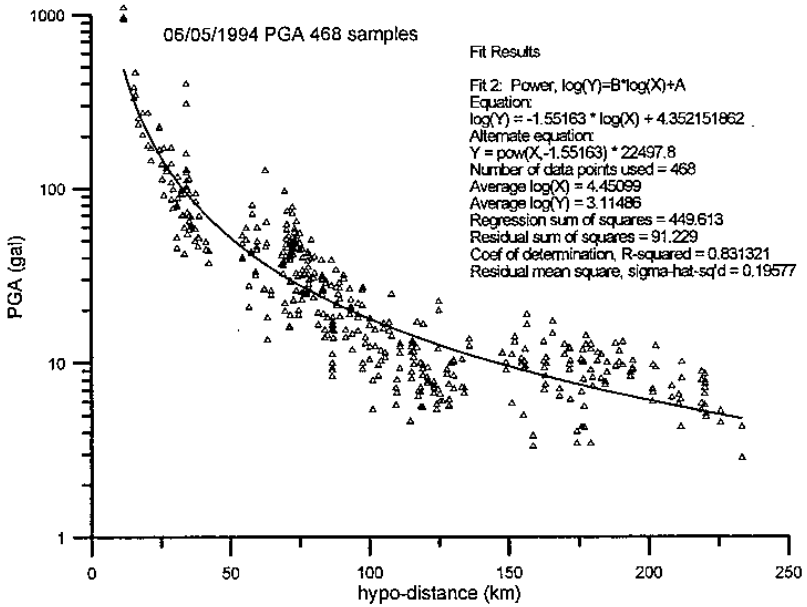

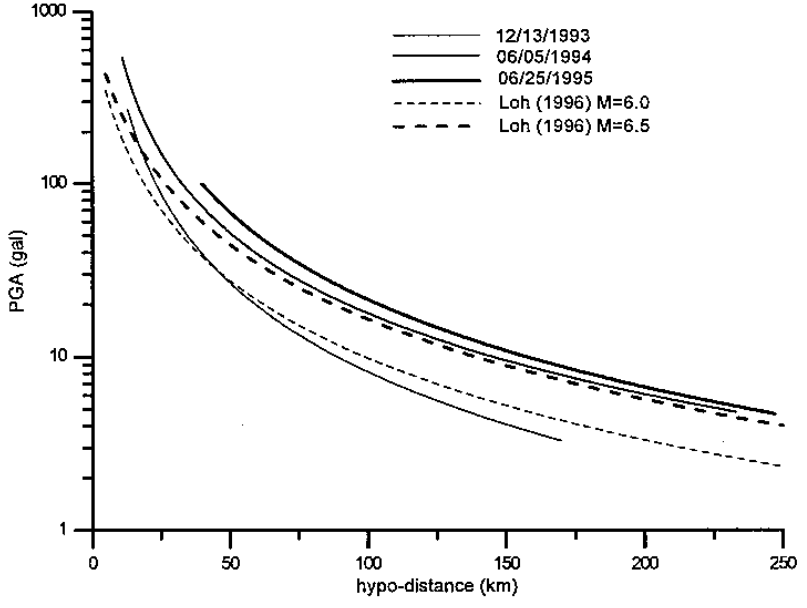

Figure 4. Logarithm of the horizontal peak ground acceleration as function of hypocentral distance: upper left for the12/15/93 earthquake, lower left for the 6/5/94 earthquake, upper right for the 6/25/95 earthquake, and lower right for the best-fit curves, respectively.

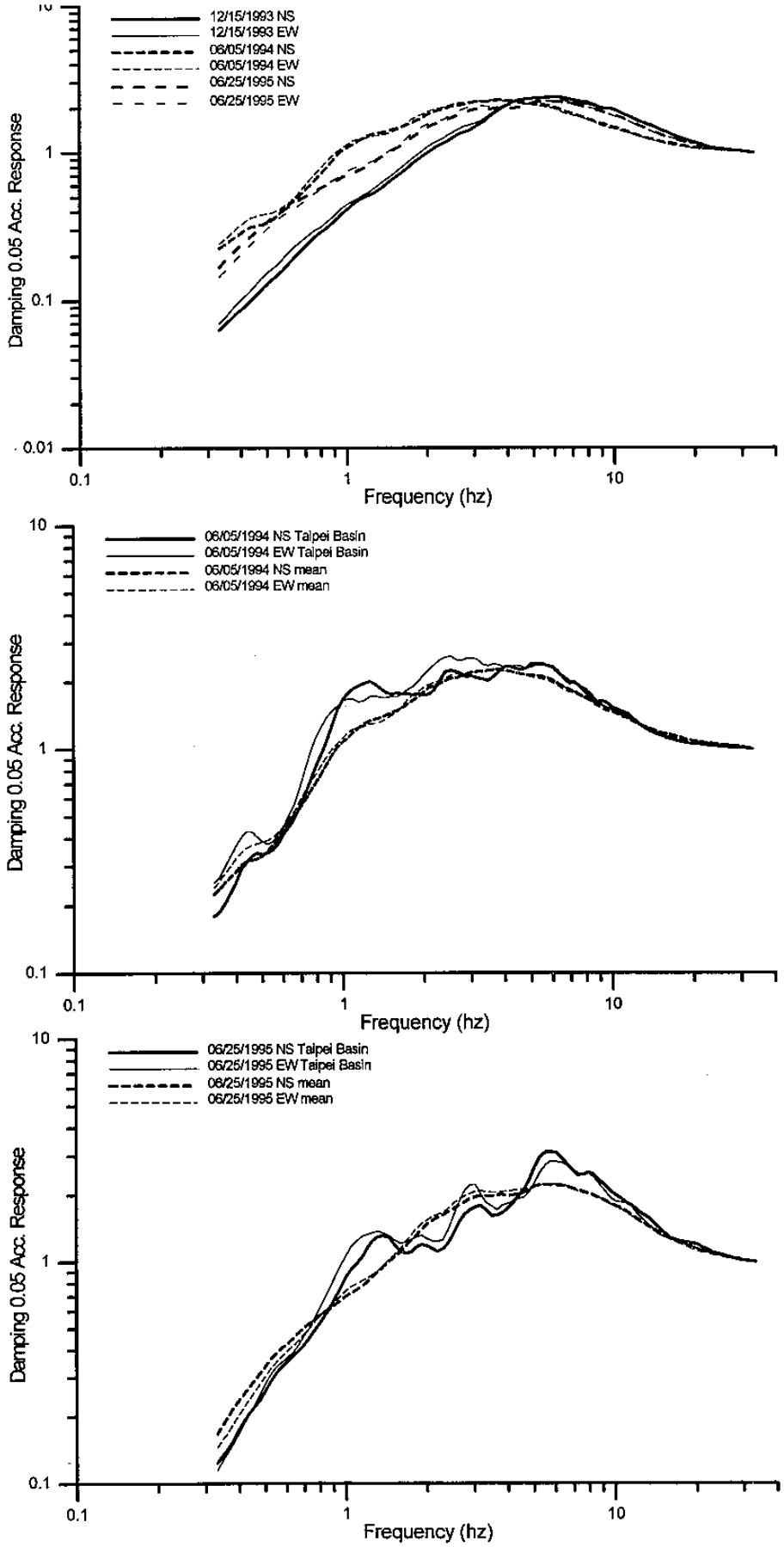

Figure 5. Average normalized acceleration response spectral shapes for 5% damping: top for the 12/15/93 earthquake, middle for the 6/5/94 earthquake, and bottom for the 6/25/95 earthquake, respectively.